



## COVID-19 Research Tools

Defeat the SARS-CoV-2 Variants

InvivoGen



### Cutting Edge: Expression of IRF8 in Gastric Epithelial Cells Confers Protective Innate Immunity against *Helicobacter pylori* Infection

This information is current as of February 26, 2022.

Ming Yan, Hongsheng Wang, Jiafang Sun, Wei Liao, Peng Li, Yin Zhu, Chengfu Xu, Jungsoo Joo, Yan Sun, Sadia Abbasi, Alexander Kovalchuk, Nonghua Lv, Warren J. Leonard and Herbert C. Morse III

*J Immunol* 2016; 196:1999-2003; Prepublished online 3 February 2016;  
doi: 10.4049/jimmunol.1500766  
<http://www.jimmunol.org/content/196/5/1999>

**Supplementary Material** <http://www.jimmunol.org/content/suppl/2016/02/02/jimmunol.1500766.DCSupplemental>

**References** This article **cites 23 articles**, 10 of which you can access for free at:  
<http://www.jimmunol.org/content/196/5/1999.full#ref-list-1>

**Why *The JI*? Submit online.**

- **Rapid Reviews! 30 days\*** from submission to initial decision
- **No Triage!** Every submission reviewed by practicing scientists
- **Fast Publication!** 4 weeks from acceptance to publication

*\*average*

**Subscription** Information about subscribing to *The Journal of Immunology* is online at:  
<http://jimmunol.org/subscription>

**Permissions** Submit copyright permission requests at:  
<http://www.aai.org/About/Publications/JI/copyright.html>

**Email Alerts** Receive free email-alerts when new articles cite this article. Sign up at:  
<http://jimmunol.org/alerts>



## Cutting Edge: Expression of IRF8 in Gastric Epithelial Cells Confers Protective Innate Immunity against *Helicobacter pylori* Infection

Ming Yan,<sup>\*,1</sup> Hongsheng Wang,<sup>†,1</sup> Jiafang Sun,<sup>†</sup> Wei Liao,<sup>‡,§</sup> Peng Li,<sup>‡,§</sup> Yin Zhu,<sup>¶</sup> Chengfu Xu,<sup>\*</sup> Jungsoo Jo,<sup>\*</sup> Yan Sun,<sup>\*</sup> Sadia Abbasi,<sup>†</sup> Alexander Kovalchuk,<sup>†</sup> Nonghua Lv,<sup>¶</sup> Warren J. Leonard,<sup>‡,§</sup> and Herbert C. Morse, III<sup>†</sup>

IFN regulatory factor 8 (IRF8) is expressed in many types of blood cells and plays critical roles in cellular differentiation and function. However, the role of IRF8 in nonhematopoietic systems remains poorly understood. In this study, we provide evidence that IRF8 is a transcriptional modulator of the gastric mucosa necessary for limiting *Helicobacter pylori* colonization. *H. pylori* infection significantly upregulated expression of IRF8, which, in turn, promoted IFN- $\gamma$  expression by gastric epithelial cells. Mice deficient in IRF8 exhibited increased *H. pylori* colonization and aborted induction of mucosal IFN- $\gamma$ . Genome-wide analyses of IFN- $\gamma$ -treated gastric epithelial cells by chromatin immunoprecipitation sequencing and RNA sequencing led to the identification of IRF8 target genes, with many belonging to the IFN-regulated gene family that was observed previously in immune cells. Our results identify the IRF8–IFN- $\gamma$  circuit as a novel gastric innate immune mechanism in the host defense against infection with *H. pylori*. *The Journal of Immunology*, 2016, 196: 1999–2003.

**I**nterferon regulatory factor (IRF)8 is a transcription factor of the IRF family with a wide range of functions in immune cell development, activation, immunomodulation, and function. Under steady-state conditions, based on an IRF8 reporter, IRF8 is expressed in developing lymphoid and myeloid cells but not in mature neutrophils, T cells, or megakaryocytes (1, 2). A knockout of the mouse gene encoding

IRF8 (*Irf8*<sup>−/−</sup> mice) results in a variety of developmental abnormalities of dendritic cells, B cells, Langerhans cells, and monocytes (reviewed in Ref. 3). IRF8 exerts its regulatory functions by binding to specific DNA sequences. Because IRF8 itself has weak DNA binding activity, heterodimerization with a partner molecule is essential to assert its transcriptional regulatory activity (4). Depending on the partner molecule, IRF8 either activates or represses expression of its target genes. Genome-wide analyses of IRF8 target genes in germinal center B cells, myeloid cells, and brain during an inflammatory response against certain pathogens revealed that IRF8 regulates a relatively conserved set of genes involved in Ag presentation, IFN responses, DNA repair, RNA expression, and protein processing (5–7).

Although IRF8 expression and function were once thought to be restricted to the hematopoietic system, more recent evidence indicates a much broader tissue distribution. Studies in the nervous system (8), heart (9), and other muscle cells (10) identified previously unrecognized functions of IRF8. For example, expression of IRF8 in neurons confers protection against ischemic-reperfusion-induced brain damage (8). Expression of IRF8 in cardiomyocytes prevents development of cardiac hypertrophy by inhibiting calcineurin signaling (9). These data underscore the importance of cell context-dependent expression and functions of IRF8. However, it remains unclear how IRF8 is regulated in these nonhematopoietic cells and what gene programs IRF8 controls.

We report that IRF8 is expressed in gastric epithelial cells (GECs), another nonhematopoietic cell type. Expression levels of IRF8 are enhanced following infection with *Helicobacter*

<sup>\*</sup>Laboratory of Biochemistry and Genetics, National Institute of Diabetes and Digestive and Kidney Diseases, National Institutes of Health, Bethesda, MD 20892; <sup>†</sup>Virology and Cellular Immunology Section, Laboratory of Immunogenetics, National Institute of Allergy and Infectious Diseases, National Institutes of Health, Rockville, MD 20852; <sup>‡</sup>Laboratory of Molecular Immunology, National Heart, Lung, and Blood Institute, National Institutes of Health, Bethesda, MD 20892; <sup>§</sup>Immunology Center, National Heart, Lung, and Blood Institute, National Institutes of Health, Bethesda, MD 20892; and <sup>¶</sup>Department of Gastroenterology, First Affiliated Hospital, Nanchang University, Nanchang 330006, China

<sup>1</sup>M.Y. and H.W. contributed equally to this work.

ORCIDs: 0000-0002-8292-6813 (S.A.); 0000-0002-9331-3705 (H.C.M.).

Received for publication April 10, 2015. Accepted for publication December 28, 2015.

This work was supported in part by the Intramural Research Programs of the National Institutes of Health, the National Institute of Allergy and Infectious Diseases (to H.W., J.S., S.A., A.K., and H.C.M.), the National Institute of Diabetes and Digestive and Kidney Diseases (to M.Y., Y.Z., J.J., Y.S., C.X., and N.L.), and the National Heart, Lung, and Blood Institute (to W.L., P.L., and W.J.L.).

The sequences presented in this article have been submitted to the National Center for Biotechnology Information Gene Expression Omnibus under accession number GSE67476.

Address correspondence and reprint requests to Dr. Herbert C. Morse, III, and Dr. Hongsheng Wang or Dr. Ming Yan, Virology and Cellular Immunology Section, Laboratory of Immunogenetics, National Institute of Allergy and Infectious Diseases, National Institutes of Health, 5640 Fishers Lane, Rockville, MD 20852 (H.C.M. and H.W.) or Laboratory of Biochemistry and Genetics, National Institute of Diabetes and Digestive and Kidney Diseases, National Institutes of Health, 8 Center Drive, Bethesda, MD 20892 (M.Y.). E-mail addresses: hmorse@niaid.nih.gov (H.C.M.) and wanghongs@niaid.nih.gov (H.W.) or yanming@mail.nih.gov (M.Y.)

The online version of this article contains supplemental material.

Abbreviations used in this article: ChIP, chromatin immunoprecipitation; ChIP-seq, ChIP sequencing; GEC, gastric epithelial cell; HSC, hematopoietic stem cell; IRF, IFN regulatory factor; qPCR, quantitative real-time PCR; RNA-seq, RNA sequencing; WT, wild-type.

Copyright © 2016 by The American Association of Immunologists, Inc. 0022-1767/16/\$30.00

*pylori*. Mice deficient in IRF8 exhibit higher bacteria loads than wild-type (WT) controls. We also show that IRF8 is induced by IFN- $\gamma$  and that IRF8, in turn, promotes IFN- $\gamma$  production, forming a positive regulative loop to amplify inflammation. Furthermore, using chromatin immunoprecipitation (ChIP) sequencing (ChIP-seq) and RNA sequencing (RNA-seq) analyses, we identified IRF8 target genes in GECs, providing a detailed understanding of how IRF8 functions in gastric mucosal innate immunity.

## Materials and Methods

### Mice and infection

B6 (WT), *Irfl8*<sup>-/-</sup>, *Irfl8*<sup>fl/fl</sup>, and IRF8-EGFP reporter mice were described previously (2, 11, 12). Vil-Cre mice (stock #4586) were purchased from The Jackson Laboratory and bred with *Irfl8*<sup>fl/fl</sup> mice to generate *Irfl8*<sup>fl/fl</sup>/Vil-Cre mice. All mice were maintained in a specific pathogen-free facility at the National Institutes of Health according to guidelines approved by the National Institute of Allergy and Infectious Diseases (ASP LIG-16) and the National Institute of Diabetes and Digestive and Kidney Diseases (NIDDK-K052-NIHMD-13) Animal Care and Use Committees. Infection of mice with the *H. pylori* SS1 strain (kindly provided by Drs. A. Lee and J. O'Rourke, University of New South Wales, Sydney, Australia) was performed as described before (13). Briefly, mice were inoculated with an oral challenge dose of 10<sup>7</sup> CFU at days 1, 3, and 5. At 4 and 8 wk following infection, stomach tissues were processed for histology and tissue culture for enumeration of *H. pylori*. For infection of cells in vitro, mouse GECs were prepared by enzyme digestion, as previously described (14). After culture for 5–8 d, subconfluent cells were incubated with *H. pylori* at a multiplicity of infection of 100 for 2 d.

### Immunohistochemistry and flow cytometry

Paraffin sections of stomach tissues were stained with a polyclonal anti-IRF8 Ab (Santa Cruz Biotechnology) and/or DAPI using standard procedures and imaged using a Nikon ECLIPSE TE2000-U confocal microscope. For intracellular staining, GECs were fixed and permeabilized using a Fix & Perm Kit (Life Technology) and stained with allophycocyanin-conjugated anti-cytokeratin Ab (pan reactive; EXBIO Praha). Cells were analyzed by a FACS LSR II flow cytometer (BD Biosciences) and FlowJo software.

### Microarray, quantitative real-time PCR, immunoblotting, RNA-seq, and ChIP-seq

Microarray analysis was done using RNA extracts from stomach tissues of infected and control mice and Affymetrix chips. Data were analyzed by the National Institute of Diabetes and Digestive and Kidney Diseases Bioinformatics facility. Quantitative real-time PCR (qPCR) was performed as described previously (15). The GSM06 GECs (a gift from Dr. Yoshiaki Tabuchi, University of Toyama) were stimulated with 10 ng/ml IFN- $\gamma$  for different times before analysis. Primers are listed in Supplemental Table I. Western blot and ChIP analyses were performed as previously described (15). ChIP-seq and RNA-seq analyses were performed as described previously (16). The sequences were submitted to the National Center for Biotechnology Information Gene Expression Omnibus under accession number GSE67476 (<http://www.ncbi.nlm.nih.gov/geo/query/acc.cgi?token=yrtwacaspzoxlqp&acc=GSE67476>).

### Statistical analysis

The unpaired two-tailed Student *t* test or Mann–Whitney *U* test was used to compare differences between two groups. The *p* values <0.05 were considered statistically significant.

## Results and Discussion

### Expression of IRF8 is increased in stomach tissues following infection with *H. pylori*

Microarray-based gene-expression profiling of gastric tissues from *H. pylori*-infected and mock-infected mice revealed a 2-fold increase in *Irfl8* transcripts in infected stomach tissues (Fig. 1A). This was confirmed by qPCR (Fig. 1B). Infection of a mouse GEC line, GSM06, with *H. pylori* also resulted in a time-dependent increase in *Irfl8* expression (Fig. 1C). Immunohistochemical analyses revealed that normal stomach

tissues expressed low levels of IRF8, as evidenced by barely positive staining of IRF8 in nucleated glandular cells (Fig. 1D). However, infection with *H. pylori* resulted in a robust increase in IRF8 in GECs (Fig. 1D). By using an IRF8-EGFP reporter mouse in which an IRF8-EGFP fusion protein is expressed under the control of natural regulatory elements of the *Irfl8* gene (2), we detected a dramatic upregulation of IRF8-EGFP expression in infected gastric glandular cells (Fig. 1E).

In an in vitro assay, cultured primary GECs of IRF8-EGFP and WT mice uniformly expressed cytokeratin, a marker of gastric epithelial identity (Fig. 1F, upper panels). Following coculture with *H. pylori*, GECs of IRF8-EGFP reporter mice, but not WT mice, upregulated expression of IRF8-EGFP (Fig. 1F, lower panels), consistent with the data from immunohistochemistry analyses. As a positive control, IFN- $\gamma$ , a known potent stimulus for IRF8 expression, significantly upregulated expression of IRF8-EGFP. The results demonstrated that IRF8 was readily induced in isolated GECs, indicating that expression induced by exposure to *H. pylori* shown in the immunohistochemistry analyses was not dependent on other gastric cell types. From this, we conclude that infection with *H. pylori* significantly increased expression of IRF8 in GECs.

### IRF8 deficiency impairs gastric innate immunity against infection with *H. pylori*

To determine whether IRF8 contributes to gastric inflammatory responses against infection with *H. pylori*, we infected *Irfl8*<sup>-/-</sup> and WT mice with the *H. pylori* SS1 strain and assessed changes in pathology and bacterial loads in stomach tissues at later time points. At 4 and 8 wk postinfection, the extent of stomach tissue damage was indistinguishable in *Irfl8*<sup>-/-</sup> and WT controls (data not shown), but bacterial loads in *Irfl8*<sup>-/-</sup> mice were significantly greater than in controls at both time points (Fig. 2A).

Because *Irfl8*<sup>-/-</sup> mice are defective in many aspects of innate and adaptive immunity, including the development and function of dendritic cells, B cells, Th17 cells, and monocytes (reviewed in Refs. 3, 17), the decreased bacterial clearance in *Irfl8*<sup>-/-</sup> mice could be due to a collective dysfunction of these immune effector cells. To gain more insights into GEC-intrinsic effects of IRF8 resulting from *H. pylori* infection, we first generated chimeric mice by reconstituting lethally irradiated *Irfl8*<sup>-/-</sup> mice with hematopoietic stem cells (HSCs) of WT mice. Eight weeks after reconstitution, the mice were infected with *H. pylori* and examined 2 mo later. *Irfl8*<sup>-/-</sup> mice reconstituted with WT HSCs still exhibited higher bacterial loads than WT control mice reconstituted with WT HSCs (Fig. 2B). Next, we generated IRF8 conditional-deletion mice using Vil-Cre-mediated deletion of the IRF8 gene in villin-expressing gastric tissues. The bacterial loads in *Irfl8*<sup>fl/fl</sup>/Vil-Cre mice were significantly higher than in *Irfl8*<sup>fl/fl</sup> control mice at both 4 and 8 wk postinfection (Fig. 2C). These data strongly support a GEC-intrinsic effect of IRF8 in limiting *H. pylori* colonization. Next, we investigated *H. pylori*-induced IFN- $\gamma$  production in GECs in vitro. Previous studies demonstrated that infection with *H. pylori* induced expression of IFN- $\gamma$  in gastric tissues (18). Consistent with this result, the expression of IFN- $\gamma$  transcripts was significantly increased in gastric tissues following *H. pylori* infection (Fig. 3A). Infection of the GSM06 GEC cell line and WT primary GECs with



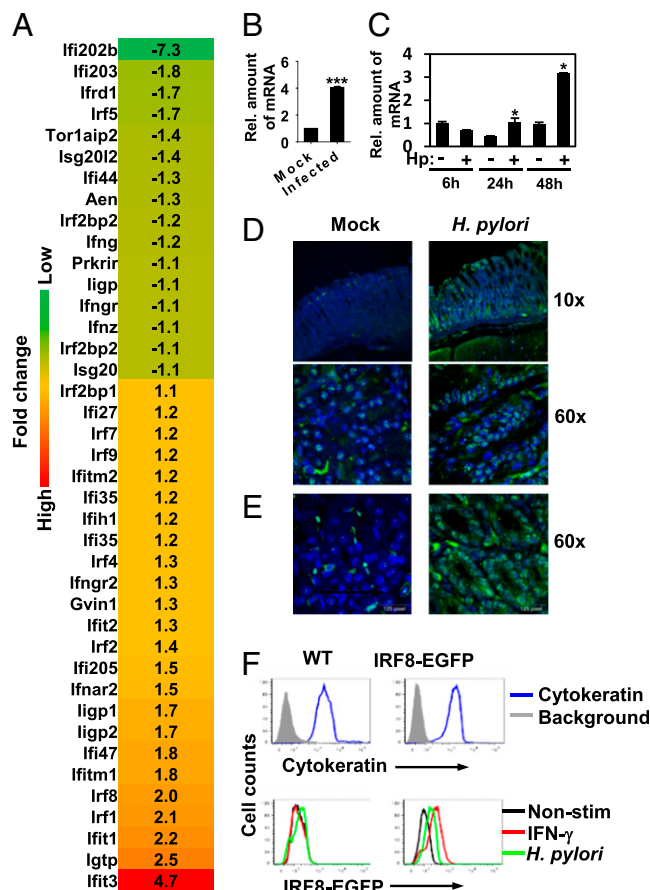


**FIGURE 1.** Expression of IRF8 in stomach. (A) Microarray analysis of IRF8 expression in stomach tissues of mice ( $n = 3$ ) infected with *H. pylori* for 2 mo. Shown are fold changes in expression of genes belonging to the IFN family and the IRF family. (B) qPCR analysis of IRF8 transcripts in stomach tissues of mice ( $n = 3$ ) infected with *H. pylori*. \*\*\* $p < 0.001$ . (C) qPCR analysis of IRF8 expression in GSM06 cells infected with *H. pylori* for different times. Error bars represent triplicate assays. Data are from one of three experiments. Fluorescence histological analysis of IRF8 expression in stomach tissues of B6 mice (D) and IRF8-EGFP reporter mice (E) infected with *H. pylori* for 8 wk. Stomach tissue sections were immunostained using indirect immunofluorescence with Abs against IRF8 (D) or direct imaging for EGFP fluorescence (E). Sections were also counterstained with DAPI (blue) to aid in the identification of nucleated cells and the localization of IRF8 to the nuclei. (D) Original magnification  $\times 10$  (top panel) and  $\times 60$ . (E) Original magnification  $\times 60$ . Data are representative of six mice per group. (F) IRF8-EGFP expression in primary GECs. Cultured GECs from WT and IRF8-EGFP mice were cocultured with *H. pylori* or IFN- $\gamma$  for 2 d and analyzed by flow cytometry. GECs stained intracellularly with anti-cytokeratin Abs to show GEC identity (upper panels). Background was determined from unstained samples. Data are representative of two independent experiments with similar results. \* $p < 0.05$ .

*H. pylori* also induced expression of IFN- $\gamma$  (Fig. 3B). However, infection failed to induce IFN- $\gamma$  expression in *Irf8*<sup>-/-</sup> GECs (Fig. 3B). Importantly, IFN- $\gamma$  transcripts were negligible or absent in gastric tissues of *Irf8*<sup>-/-</sup> mice infected with *H. pylori* for 4 and 8 wk (Fig. 3C). Taken together, these data suggest that expression of IFN- $\gamma$  in *H. pylori*-infected GECs is IRF8 dependent.

#### IFN- $\gamma$ contributes to *H. pylori*-induced inflammation and regulates expression of IRF8

As noted previously, IFN- $\gamma$  is a potent inducer of IRF8 expression in immune cells (19). Interestingly, IFN- $\gamma$  also induced IRF8 expression in GSM06 cells in a time-dependent

manner (Fig. 3D). Similarly, stimulation of primary GECs of IRF8-EGFP mice with IFN- $\gamma$  also increased IRF8-EGFP expression (Fig. 1F, lower panels). It is worth noting that GECs express IFN- $\gamma$  receptors constitutively, as determined by qPCR analyses of transcript levels for the IFN- $\gamma$  receptors *Ifngr1* and *Ifngr2* (data not shown). Taken together, these data suggested that IFN- $\gamma$  drives IRF8 expression, which, in turn, promotes IFN- $\gamma$  production. This positive-feedback loop is expected to amplify IFN- $\gamma$ -mediated immunity in the early phase of infection, which could change the course of later adaptive immunity to *H. pylori* by priming CD4<sup>+</sup> T cells for Th1 differentiation (reviewed in Ref. 20).

#### IRF8 controls expression of a large number of genes in GECs

Previous high-throughput genomic analyses of tissue-specific IRF8 target genes in stomachs were based on analyses of whole tissues, obviating the opportunity to discern the contributions of gastric cells versus infiltrated inflammatory immune cells, which often express high levels of IRF8 (2). To overcome this obstacle, we performed genome-wide analysis of IRF8 target genes using ChIP-seq and RNA-seq and the GEC line (GSM06) stimulated with IFN- $\gamma$ , a factor that was more efficient than *H. pylori* in inducing IRF8 protein expression (Fig. 1F), enabling us to generate high-quality ChIP materials for analysis. To demonstrate that this approach is relevant to the biology of a true infection, we validated some of the target genes identified following IFN- $\gamma$  treatment using cultured mouse primary GECs infected with *H. pylori*.

We identified 666 IRF8-specific ChIP-seq peaks in DNA from cells stimulated with IFN- $\gamma$ . The distribution of IRF8 binding sites, with 20% proximal to the transcription start

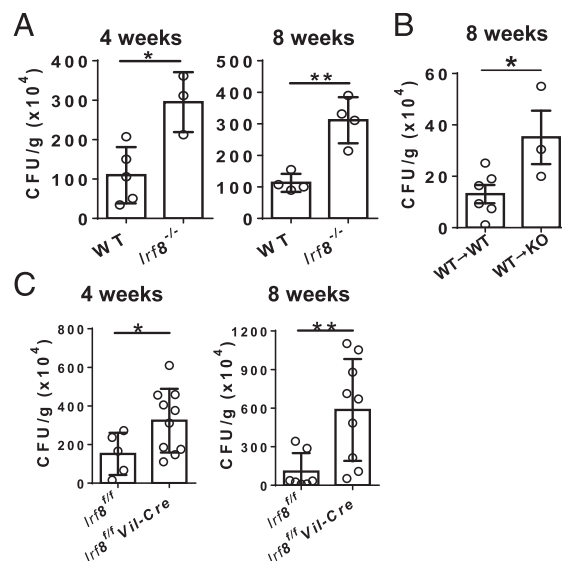


**FIGURE 2.** IRF8 deficiency impaired bacterial clearance in the stomach. (A) *Irf8*<sup>-/-</sup> and WT mice were infected with *H. pylori* for 4 and 8 wk and analyzed for bacterial load. Each symbol represents a mouse. (B) Lethally irradiated WT and *Irf8*<sup>-/-</sup> mice reconstituted with WT HSCs for 2 mo were infected with *H. pylori* for 8 wk and analyzed for bacterial load as in (A). Each symbol represents a mouse. Data are pooled from two experiments. (C) *Irf8*<sup>fl/fl</sup> Vil-Cre mice were infected with *H. pylori* as in (A). Each symbol represents a mouse. \* $p < 0.05$ , \*\* $p < 0.01$ .

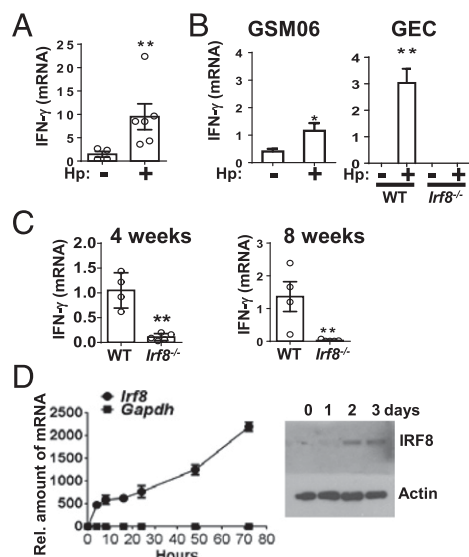


**FIGURE 3.** IFN- $\gamma$  and IRF8 expression in stomach tissues. (A) Stomach tissues of WT mice infected with *H. pylori* for 8 wk were analyzed by qPCR for IFN- $\gamma$  expression. Each symbol represents a mouse. (B) IFN- $\gamma$  expression in GSM06 cells and primary GECs of WT and *Irif8*<sup>-/-</sup> mice infected with *H. pylori* for 24 h. Error bars are for triplicate assays. Data are representative of two independent experiments. (C) IFN- $\gamma$  expression in stomach tissues of *Irif8*<sup>-/-</sup> and WT mice infected with *H. pylori* for 4 and 8 wk. Each symbol represents a mouse. (D) GSM06 cells were stimulated with IFN- $\gamma$  for 24 h. IRF8 expression was analyzed by qPCR (left panel) and immunoblotting (right panel). Data represent three independent experiments. \*\**p* < 0.01.

site, 32% intronic, and 35% intergenic (Fig. 4A), was similar to that recently described for IRF8-induced mouse monocyte differentiation (21). De novo motif analysis revealed that IRF8-bound genomic sequences were greatly enriched (71%) for the sequence, GAAANNGAAA, which matches the core consensus IFN-stimulated response element sequence (Fig. 4B). Of the 666 IRF8 ChIP-seq peaks, 314 bound within genes annotated by RefSeq (Fig. 4C).

RNA-seq analyses of gene expression by the IFN- $\gamma$ -stimulated and control cells identified 1037 IFN- $\gamma$ -regulated genes, including 605 that were upregulated and 432 that were downregulated (Fig. 4D). The overlap of IRF8-bound genes identified by ChIP-seq with IFN- $\gamma$ -stimulated genes identified by RNA-seq included 77 genes: 73 were upregulated, and 4 were downregulated (Fig. 4C, Supplemental Table II). Ingenuity functional analysis revealed that 48% of these genes are involved in endocrine system disorders, gastrointestinal diseases, and immunological diseases, whereas 41% of these genes belong to pathways of antimicrobial response, inflammatory response, and endocrine system disorders (Supplemental Table II). Interestingly, the most increased gene (*Ifit3*), but not the most decreased gene (*Ifi202b*), in infected gastric tissues (Fig. 1A) was found to be a direct target of IRF8 (Supplemental Table II). *Ifit3* was recently identified as a novel antiviral protein (22, 23) and could be an important innate factor against microbial infection.

Previous gene microarray profiling analysis in the lungs of *Mycobacterium tuberculosis*-infected mice and ChIP-seq analysis in the brain of malaria-infected mice led to the identification of a common core of 53 IRF8-bound genes that were upregulated in both conditions (5). Given that different tissues express significantly different gene profiles and that

IRF8 targets can vary with tissue, this core list could be an underestimate. Nevertheless, we compared this “common core” list with our 77-gene list and identified 17 genes that overlapped in all three tissues. These genes ontologically belong to innate immunity (*Ifit3*, *Nlr5*, *Oasl2*, *Trim21*), adaptive immunity, Ag processing and presentation (*Cd274*, *H2-T22*, *Psm8*, *Tap2*), GTP signaling (*Gbp2*, *Gbp3*, *Igtg*, *Irgm1*, *Irgm2*), and ubiquitination (*Rnf19b*, *Usp18*). The small number of overlapping genes also indicates that IRF8-controlled gene programs are mostly cell context dependent.

To determine whether IRF8 is required for expression of these genes, we analyzed expression of *Usp18*, *Upp1*, *Nlr5*, *Ifit3*, *Ifit1*, and *Ifi35* in primary GECs of WT and *Irif8*<sup>-/-</sup> mice. The cells were treated with IFN- $\gamma$  or infected with *H. pylori* for 2 d, and gene-expression levels were analyzed by qPCR. As shown in Fig. 4E, transcript levels of all six genes were significantly higher in primary GECs of WT mice than in IRF8-deficient controls following stimulation with IFN- $\gamma$  (Fig. 4E, *p* < 0.001). As expected, deficiency in IRF8 abrogated *H. pylori*-induced upregulation of these genes (Fig. 4E). In addition, the degree of altered gene

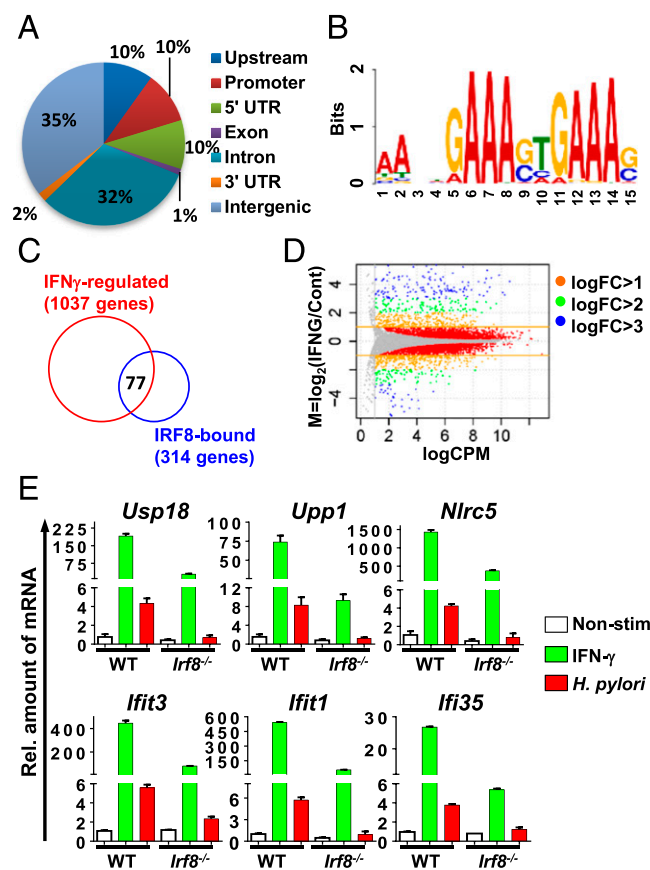


**FIGURE 4.** Genome-wide analysis of IRF8 targets in GECs. (A) Genomic binding distribution of IRF8 binding induced by IFN- $\gamma$  (upstream: [−15 kb, −5 kb], promoter: [−5 kb, transcription start site]). (B) De novo motif analysis indicated that 474 of 666 binding sites contained the IRF core motif GAAANNGAAA. (C) Seventy-seven genes are bound by IRF8 and also differentially expressed following stimulation with IFN- $\gamma$ . (D) RNA-seq analysis shows that IFN- $\gamma$  regulated a number of genes, including 605 that were upregulated and 432 that were downregulated (false-discovery rate < 0.05, fold change [FC] > 2). (E) IRF8-bound genes, including *USP18*, *Upp1*, *Nlr5*, *Ifit1*, *Ifit3*, and *Ifi35* are stimulated by IFN- $\gamma$  and *H. pylori* in an IRF8-dependent fashion. The primary GECs of WT and *Irif8*<sup>-/-</sup> stomach tissues were cocultured with *H. pylori* or IFN- $\gamma$  for 2 d. Data represent two independent experiments.

expression in IFN- $\gamma$ -treated GECs was significantly greater than in *H. pylori*-infected GECs, suggesting that IFN- $\gamma$  is a prominent stimulator for elicitation of robust GEC gene-expression programs.

Previous studies support a Th1-biased adaptive immune response during *H. pylori*-induced gastric infection (20). Our study extends this view by providing new evidence that infected GECs exhibit an IRF8-IFN- $\gamma$ <sup>+</sup> regulatory circuit that would facilitate Th1 cell differentiation. Because GECs produce IFN- $\gamma$  (Fig. 3) (14), and IFN- $\gamma$  expression in GECs is completely dependent on IRF8 (Fig. 3), these data suggest that IRF8 could be the major regulator for IFN- $\gamma$  production in infected gastric tissues. Importantly, the IRF8-IFN- $\gamma$  regulatory circuit may amplify local inflammatory responses to promote bacterial clearance. Thus, it is possible that downregulation of IRF8 in GECs may facilitate chronic infection and enhance the likelihood of *H. pylori*-induced malignant transformation.

## Acknowledgments

We thank Alfonso Macias for maintaining the mouse colony. This article is dedicated to the memory of Dr. William G. Coleman, Jr., who initiated and supervised this collaborative study with H.C.M. and H.W.

## Disclosures

The authors have no financial conflicts of interests.

## References

- Schönheit, J., C. Kuhl, M. L. Gebhardt, F. F. Klett, P. Riemke, M. Scheller, G. Huang, R. Naumann, A. Leutz, C. Stocking, et al. 2013. PU.1 level-directed chromatin structure remodeling at the *Irf8* gene drives dendritic cell commitment. *Cell Reports* 3: 1617–1628.
- Wang, H., M. Yan, J. Sun, S. Jain, R. Yoshimi, S. M. Abolfath, K. Ozato, W. G. Coleman, Jr., A. P. Ng, D. Metcalf, et al. 2014. A reporter mouse reveals lineage-specific and heterogeneous expression of IRF8 during lymphoid and myeloid cell differentiation. *J. Immunol.* 193: 1766–1777.
- Wang, H., and H. C. Morse, III. 2009. IRF8 regulates myeloid and B lymphoid lineage diversification. *Immunol. Res.* 43: 109–117.
- Taylor, P., T. Tamura, H. C. Morse, III, and K. Ozato. 2008. The BXH2 mutation in IRF8 differentially impairs dendritic cell subset development in the mouse. *Blood* 111: 1942–1945.
- Berghout, J., D. Langlais, I. Radovanovic, M. Tam, J. D. MacMicking, M. M. Stevenson, and P. Gros. 2013. *Irf8*-regulated genomic responses drive pathological inflammation during cerebral malaria. *PLoS Pathog.* 9: e1003491–e1003505.
- Marquis, J. F., O. Kapoustina, D. Langlais, R. Ruddy, C. R. Dufour, B. H. Kim, J. D. MacMicking, V. Giguère, and P. Gros. 2011. Interferon regulatory factor 8 regulates pathways for antigen presentation in myeloid cells and during tuberculosis. *PLoS Genet.* 7: e1002097–e1002111.
- Shin, D. M., C. H. Lee, and H. C. Morse, III. 2011. IRF8 governs expression of genes involved in innate and adaptive immunity in human and mouse germinal center B cells. *PLoS One* 6: e27384.
- Xiang, M., L. Wang, S. Guo, Y. Y. Lu, H. Lei, D. S. Jiang, Y. Zhang, Y. Liu, Y. Zhou, X. D. Zhang, and H. Li. 2014. Interferon regulatory factor 8 protects against cerebral ischaemic-reperfusion injury. *J. Neurochem.* 129: 988–1001.
- Jiang, D. S., X. Wei, X. F. Zhang, Y. Liu, Y. Zhang, K. Chen, L. Gao, H. Zhou, X. H. Zhu, P. P. Liu, et al. 2014. IRF8 suppresses pathological cardiac remodelling by inhibiting calcineurin signalling. *Nat. Commun.* 5: 3303–3317.
- Zhang, S. M., L. Gao, X. F. Zhang, R. Zhang, L. H. Zhu, P. X. Wang, S. Tian, D. Yang, K. Chen, L. Huang, et al. 2014. Interferon regulatory factor 8 modulates phenotypic switching of smooth muscle cells by regulating the activity of myocardin. *Mol. Cell Biol.* 34: 400–414.
- Holtschke, T., J. Löhler, Y. Kanno, T. Fehr, N. Giese, F. Rosenbauer, J. Lou, K. P. Knobloch, L. Gabriele, J. F. Waring, et al. 1996. Immunodeficiency and chronic myelogenous leukemia-like syndrome in mice with a targeted mutation of the ICSBP gene. *Cell* 87: 307–317.
- Feng, J., H. Wang, D. M. Shin, M. Masiuk, C. F. Qi, and H. C. Morse, III. 2011. IFN regulatory factor 8 restricts the size of the marginal zone and follicular B cell pools. *J. Immunol.* 186: 1458–1466.
- Algood, H. M., J. Gallo-Romero, K. T. Wilson, R. M. Peek, Jr., and T. L. Cover. 2007. Host response to *Helicobacter pylori* infection before initiation of the adaptive immune response. *FEMS Immunol. Med. Microbiol.* 51: 577–586.
- Lina, T. T., I. V. Pinchuk, J. House, Y. Yamaoka, D. Y. Graham, E. J. Beswick, and V. E. Reyes. 2013. CagA-dependent downregulation of B7-H2 expression on gastric mucosa and inhibition of Th17 responses during *Helicobacter pylori* infection. *J. Immunol.* 191: 3838–3846.
- Lee, C. H., M. Melchers, H. Wang, T. A. Torrey, R. Slota, C. F. Qi, J. Y. Kim, P. Luga, H. J. Kong, L. Farrington, et al. 2006. Regulation of the germinal center gene program by interferon (IFN) regulatory factor 8/IFN consensus sequence-binding protein. *J. Exp. Med.* 203: 63–72.
- Ring, A. M., J. X. Lin, D. Feng, S. Mitra, M. Rickert, G. R. Bowman, V. S. Pande, P. Li, I. Moraga, R. Spolski, et al. 2012. Mechanistic and structural insight into the functional dichotomy between IL-2 and IL-15. *Nat. Immunol.* 13: 1187–1195.
- Ouyang, X., R. Zhang, J. Yang, Q. Li, L. Qin, C. Zhu, J. Liu, H. Ning, M. S. Shin, M. Gupta, et al. 2011. Transcription factor IRF8 directs a silencing programme for TH17 cell differentiation. *Nat. Commun.* 2: 314–326.
- Lindholm, C., M. Quiding-Jarbrink, H. Lönroth, A. Hamlet, and A. M. Svennerholm. 1998. Local cytokine response in *Helicobacter pylori*-infected subjects. *Infect. Immun.* 66: 5964–5971.
- Kanno, Y., B. Z. Levi, T. Tamura, and K. Ozato. 2005. Immune cell-specific amplification of interferon signaling by the IRF-4/8-PU.1 complex. *J. Interferon Cytokine Res.* 25: 770–779.
- Velin, D., and P. Michetti. 2006. Immunology of *Helicobacter pylori* infection. *Digestion* 73: 116–123.
- Kurotaki, D., N. Osato, A. Nishiyama, M. Yamamoto, T. Ban, H. Sato, J. Nakabayashi, M. Umehara, N. Miyake, N. Matsumoto, et al. 2013. Essential role of the IRF8-KLF4 transcription factor cascade in murine monocyte differentiation. *Blood* 121: 1839–1849.
- Liu, X. Y., W. Chen, B. Wei, Y. F. Shan, and C. Wang. 2011. IFN-induced TPR protein IFIT3 potentiates antiviral signaling by bridging MAVS and TBK1. *J. Immunol.* 187: 2559–2568.
- Schmeisser, H., J. Mejido, C. A. Balinsky, A. N. Morrow, C. R. Clark, T. Zhao, and K. C. Zoon. 2010. Identification of alpha interferon-induced genes associated with antiviral activity in Daudi cells and characterization of IFIT3 as a novel antiviral gene. *J. Virol.* 84: 10671–10680.